

## **SCATTERING FROM BODIES COATED WITH METAMATERIAL USING FDFD METHOD**

**S. H. Zainud-Deen**

Faculty of Electronic Engineering  
Menoufia University  
Menouf, Egypt

**A. Z. Botros and M. S. Ibrahim**

Faculty of Engineering  
Cairo University  
Cairo, Egypt

**Abstract**—The electromagnetic scattering from a conducting object coated with metamaterials, which have both negative permittivity and permeability is derived rigorously by using finite difference frequency domain (FDFD). A formulation for the FDFD method is presented. The scattering from circular and multilayers elliptic cylinder coated by metamaterial are investigated. Also, the scattering from dielectric and metamaterial sphere is depicted. Numerical results are compared with the available data in the literature.

### **1. INTRODUCTION**

Metamaterials are materials with negative permittivity and permeability within certain frequency range. Moreover, the advent of metamaterials, i.e. engineered materials synthesized by including suitable particles in a host medium that lead to exciting electromagnetic properties otherwise not easily available in nature, have opened new possibilities to researchers and designers working on the enhancement of component performances, usually limited by some physical constraints when standard materials are employed [1]. Metamaterials, with simultaneously negative permittivity and permeability have received intensive interests, which exhibit a lot of exotic properties as reversal Doppler shift and negative refraction index. The concepts of critical and Brewster angles are well established in electromagnetic theory. Yet, the recent

advent of a new class of metamaterials exhibiting negative constitutive parameters reveals that these fundamental concepts should be revisited since media now exist wherein waves are totally reflected when propagating at angles below the critical angle, and transmitted when propagating at angles above the critical angle. In addition, within the region of transmission, a Brewster angle might exist in some cases, yielding an inversion of critical angle and Brewster angle, namely the Brewster angle appears beyond the critical angle, and not below like it is currently well-accepted [2–4].

Scattering of electromagnetic waves by complex-shaped metamaterial objects is an interesting research subject to develop potential application of this artificial material. The electromagnetic scattering from single and array of cylinders coated by metamaterials, which have both negative permittivity and permeability, for both normal and oblique incidence had been studied in [5–8]. Only two-dimensional cases are considered.

In this paper, the electromagnetic scattering from objects coated by metamaterials is investigated. Two- and three-dimensional objects are considered. The Finite-Difference Frequency-Domain (FDFD) method is formulated for the objects coated with metamaterial and used to calculate the scattering from different objects and compared with the available published results. The FDFD is simplest in formulation and most flexible in modeling arbitrarily shaped inhomogeneously filled and anisotropic scatterers [9–12].

## 2. THEORETICAL BACKGROUND

### Finite-Difference Frequency-Domain Technique for Metamaterials:

Considering a region of space that is source free, but may have materials that absorb electric or magnetic field energy, then Maxwell's curl equations in frequency domain are

$$\nabla \times \bar{E}_{total} = -j\omega\mu\bar{H}_{total} - \sigma^* H_{total} = -jn k_o \eta \left( 1 + \frac{\sigma^*}{jn k_o \eta} \right) H_{total}, \quad (1a)$$

and

$$\nabla \times \bar{H}_{total} = (j\omega\varepsilon + \sigma) \bar{E}_{total} = j \frac{nk_o}{\eta} \left( 1 + \frac{\sigma}{j \frac{nk_o}{\eta}} \right) \bar{E}_{total} \quad (1b)$$

The wave number and intrinsic impedance for the object are:

$$\begin{aligned} k &= nk_o \\ n &= +\sqrt{\mu_r \varepsilon_r} \quad \text{for dielectric object,} \\ n &= -\sqrt{\mu_r \varepsilon_r} \quad \text{for Metamaterial object} \end{aligned}$$

Define the total fields as sum of incident and scattered fields:

$$\overline{E}_{total} = \overline{E}^{inc} + \overline{E}^{scat}, \quad \text{and} \quad \overline{H}_{total} = \overline{H}^{inc} + \overline{H}^{scat} \quad (2)$$

where  $\overline{E}^{inc}$ , and  $\overline{E}^{scat}$  are the incident and the scattered field respectively. The incident field is the field which propagates in computation domain when no scatters exist. If the background of the computation domain is free space, then Maxwell's curl equations can be rewritten as:

$$\nabla_x \overline{E}^{scat} + jnk_o \eta \left( 1 + \frac{\sigma^*}{jnk_o \eta} \right) \overline{H}^{scat} = \left[ jk_o \eta_o - jnk_o \eta \left( 1 + \frac{\sigma^*}{jnk_o \eta} \right) \overline{H}^{inc} \right] \quad (3)$$

$$\nabla_x \overline{H}^{scat} - j \frac{nk_o}{\eta} \left( 1 + \frac{\sigma}{j \frac{nk_o}{\eta}} \right) \overline{E}^{scat} = \left[ -j \frac{k_o}{\eta_o} + j \frac{nk_o}{\eta} \left( 1 + \frac{\sigma}{j \frac{nk_o}{\eta}} \right) \right] \overline{E}^{inc} \quad (4)$$

Maxwell's equations can be reduced to two sets of scalar equations (i.e., TM<sub>z</sub> and TE<sub>z</sub>) in two dimensional case.

Using the central difference algorithm to solve for the space derivatives, Yee introduced his algorithm [13], in 1966 to solve Maxwell's partial differential equations. Yee discretized the space of the problem to small cubical cells (rectangular cells in 2D case) and for each cell he locates the six field components to match the curl equations. Discrete equations given below are obtained by replacing derivatives in these equations with their finite-difference approximations. At the boundaries of the computational domain, the perfectly matched layer boundary condition (PML) is used to absorb all the outgoing radiation. The derivation of the PML is discussed in details by Berenger [14].

#### For the TM Case:

The FDFD iterative equations are

$$H_x^{scat}(i, j) = \frac{1}{jn(i, j)k_o \eta_{xy}(i, j) \left( 1 + \frac{\sigma_{xy}^*(i, j)}{jn(i, j)k_o \eta_{xy}(i, j)} \right)} \frac{E_z^{scat}(i, j) - E_z^{scat}(i, j + 1)}{\Delta y} +$$

$$\frac{\left(\eta_o - n(i, j)\eta_{xi}(i, j) \left(1 + \frac{\sigma_{xi}^*(i, j)}{jn(i, j)k_o\eta_{xi}(i, j)}\right)\right)}{n(i, j)\eta_{xi}(i, j) \left(1 + \frac{\sigma_{xi}^*(i, j)}{jn(i, j)k_o\eta_{xi}(i, j)}\right)} H_x^{inc}(i, j) \quad (5)$$

$$H_y^{scat}(i, j) = \frac{1}{jn(i, j)k_o\eta_{yx}(i, j) \left(1 + \frac{\sigma_{yx}^*(i, j)}{jn(i, j)k_o\eta_{yx}(i, j)}\right)} \frac{E_z^{scat}(i+1, j) - E_z^{scat}(i, j)}{\Delta x} + \frac{\left(\eta_o - n(i, j)\eta_{yi}(i, j) \left(1 + \frac{\sigma_{yi}^*(i, j)}{jn(i, j)k_o\eta_{yi}(i, j)}\right)\right)}{n(i, j)\eta_{yi}(i, j) \left(1 + \frac{\sigma_{yi}^*(i, j)}{jn(i, j)k_o\eta_{yi}(i, j)}\right)} H_y^{inc}(i, j) \quad (6)$$

$$E_z^{scat}(i, j) + \frac{H_y^{scat}(i-1, j) - H_y^{scat}(i, j)}{j \frac{n(i, j)k_o}{\eta_{zx}(i, j)} \left(1 + \frac{\sigma_{zx}(i, j)}{j \frac{n(i, j)k_o}{\eta_{zx}(i, j)}}\right) \omega \varepsilon_{zx}(i, j) \Delta x} + \frac{H_x^{scat}(i, j) - H_x^{scat}(i, j-1)}{j \frac{n(i, j)k_o}{\eta_{zy}(i, j)} \left(1 + \frac{\sigma_{zy}(i, j)}{j \frac{n(i, j)k_o}{\eta_{zy}(i, j)}}\right) \omega \varepsilon_{zx}(i, j) \Delta y} = \frac{\left[\eta_{zi} - n(i, j)\eta_o(i, j) \left(1 + \frac{\sigma_{zi}(i, j)}{j \frac{n(i, j)k_o}{\eta_{zi}(i, j)}}\right)\right]}{n(i, j)\eta_o(i, j) \left(1 + \frac{\sigma_{zi}(i, j)}{j \frac{n(i, j)k_o}{\eta_{zi}(i, j)}}\right)} E_z^{inc}(i, j) \quad (7)$$

then

$$a(i, j)E_z^{scat}(i+1, j) + b(i, j)E_z^{scat}(i-1, j) + c(i, j)E_z^{scat}(i, j+1) + d(i, j)E_z^{scat}(i, j-1) + e(i, j)E_z^{scat}(i, j) = f(i, j) \quad (8)$$

where

$$a(i, j) = \frac{\eta_{zx}(i, j)}{(k_o \Delta x n(i, j))^2 \eta_{yx}(i, j) \left(1 + \frac{\sigma_{zx}(i, j)}{j \frac{n(i, j)k_o}{\eta_{zx}(i, j)}}\right) \left(1 + \frac{\sigma_{yx}^*(i, j)}{jn(i, j)k_o\eta_{yx}(i, j)}\right)}$$

$b(i, j) =$

$$\frac{\eta_{zx}(i, j)}{(k_o \Delta x)^2 n(i, j) n(i-1, j) \eta_{yx}(i-1, j) \left(1 + \frac{\sigma_{zx}(i, j)}{j \frac{n(i, j)k_o}{\eta_{zx}(i, j)}}\right) \left(1 + \frac{\sigma_{yx}^*(i-1, j)}{jn(i-1, j)k_o\eta_{yx}(i-1, j)}\right)}$$

$$c(i, j) = \frac{\eta_{zy}(i, j)}{(k_o \Delta y)^2 n(i, j) n(i, j) \eta_{xy}(i, j) \left(1 + \frac{\sigma_{zy}(i, j)}{j \frac{n(i, j) k_o}{\eta_{zy}(i, j)}}\right) \left(1 + \frac{\sigma_{xy}^*(i, j)}{jn(i, j) k_o \eta_{xy}(i, j)}\right)}$$

$$d(i, j) = \frac{\eta_{zy}(i, j)}{(k_o \Delta y)^2 n(i, j) n(i, j-1) \eta_{xy}(i, j-1) \left(1 + \frac{\sigma_{zy}(i, j)}{j \frac{n(i, j) k_o}{\eta_{zy}(i, j)}}\right) \left(1 + \frac{\sigma_{xy}^*(i, j-1)}{jn(i, j-1) k_o \eta_{xy}(i, j-1)}\right)}$$

$$e(i, j) = 1 - a(i, j) - b(i, j) - c(i, j) - d(i, j),$$

and

$$\begin{aligned} f(i, j) = & \frac{\eta_{zi}(i, j) - n(i, j) \eta_o \left(1 + \frac{\sigma_{zi}(i, j)}{j \frac{n(i, j) k_o}{\eta_{zi}(i, j)}}\right)}{n(i, j) \eta_o \left(1 + \frac{\sigma_{zi}(i, j)}{j \frac{n(i, j) k_o}{\eta_{zi}(i, j)}}\right)} E_z^{inc}(i, j) - \\ & \frac{(\eta_o - n(i, j) \eta_{yi}(i, j)) \left(1 + \frac{\sigma_{yi}^*(i, j)}{jn(i, j) k_o \eta_{yi}(i, j)}\right)}{j \frac{n(i, j) k_o \Delta x}{\eta_{zx}(i, j)} \left(1 + \frac{\sigma_{zx}(i, j)}{j \frac{n(i, j) k_o}{\eta_{zx}(i, j)}}\right) n(i, j) \eta_{yi}(i, j) \left(1 + \frac{\sigma_{yi}^*(i, j)}{jn(i, j) k_o \eta_{yi}(i, j)}\right)} H_y^{inc}(i, j) - \\ & \frac{(\eta_o - n(i-1, j) \eta_{yi}(i-1, j)) \left(1 + \frac{\sigma_{yi}^*(i-1, j)}{jn(i-1, j) k_o \eta_{yi}(i-1, j)}\right)}{j \frac{n(i, j) k_o \Delta x}{\eta_{zx}(i, j)} \left(1 + \frac{\sigma_{zx}(i, j)}{j \frac{n(i, j) k_o}{\eta_{zx}(i, j)}}\right) n(i-1, j) \eta_{yi}(i-1, j) \left(1 + \frac{\sigma_{yi}^*(i-1, j)}{jn(i-1, j) k_o \eta_{yi}(i-1, j)}\right)} H_y^{inc}(i-1, j) + \\ & \frac{(\eta_o - n(i, j) \eta_{xi}(i, j)) \left(1 + \frac{\sigma_{xi}^*(i, j)}{jn(i, j) k_o \eta_{xi}(i, j)}\right)}{j \frac{n(i, j) k_o \Delta y}{\eta_{zy}(i, j)} \left(1 + \frac{\sigma_{zy}(i, j)}{j \frac{n(i, j) k_o}{\eta_{zy}(i, j)}}\right) n(i, j) \eta_{xi}(i, j) \left(1 + \frac{\sigma_{xi}^*(i, j)}{jn(i, j) k_o \eta_{xi}(i, j)}\right)} H_x^{inc}(i, j) + \\ & \frac{(\eta_o - n(i, j-1) \eta_{xi}(i, j-1)) \left(1 + \frac{\sigma_{xi}^*(i, j-1)}{jn(i, j-1) k_o \eta_{xi}(i, j-1)}\right)}{j \frac{n(i, j) k_o \Delta y}{\eta_{zy}(i, j)} \left(1 + \frac{\sigma_{zy}(i, j)}{j \frac{n(i, j) k_o}{\eta_{zy}(i, j)}}\right) n(i, j-1) \eta_{xi}(i, j-1) \left(1 + \frac{\sigma_{xi}^*(i, j-1)}{jn(i, j-1) k_o \eta_{xi}(i, j-1)}\right)} H_x^{inc}(i, j-1) \end{aligned}$$

**Out of the PML Region:**

$$\eta_{xy} = \eta_x, \sigma_{xy}^* = \sigma_x^*, \eta_{xi} = \eta_x, \sigma_{xi}^* = \sigma_x^*, \eta_{yx} = \eta_y, \sigma_{yx}^* = \sigma_y^*, \eta_{yi} = \eta_y,$$

$$\sigma_{yi}^* = \sigma_y^*, \eta_{zx} = \eta_z, \sigma_{zx} = \sigma_z, \eta_{zy} = \eta_z, \sigma_{zy} = \sigma_z, \eta_{zi} = \eta_z, \text{ and } \sigma_{zi} = \sigma_z$$

**and in PML Region:**

$$\eta_{xy} = \eta_o, \sigma_{xy}^* = \sigma_y^m, \eta_{xi} = \frac{\eta_o}{n}, \sigma_{xi}^* = 0, \eta_{yx} = \eta_o, \sigma_{yx}^* = \sigma_x^m, \eta_{yi} = \frac{\eta_o}{n},$$

$\sigma_{yi}^* = 0$ ,  $\eta_{zx} = \eta_o$ ,  $\sigma_{zx} = \sigma_x^e$ ,  $\eta_{zy} = \eta_o$ ,  $\sigma_{zy} = \sigma_y^e$ ,  $\eta_{zi} = n\eta_o$ , and  $\sigma_{zi} = 0$   
 $\sigma^e$ ,  $\sigma^m$ : are electric and magnetic conductivity distributions in PML layer respectively,  $\frac{\sigma^e}{\varepsilon} = \frac{\sigma^m}{\mu}$  for perfect matching between free space and the PML region, and

$$\sigma^{e,m}(h) = \sigma_{\max} \left( \frac{h}{\delta_{PML}} \right)^{n+1}$$

where  $\sigma_{\max} = -\frac{\varepsilon_o c(n+1) \ln[R(0)]}{2\delta_{PML}}$ ,  $\sigma_{\max}$ : is the maximum conductivity,  $\delta_{PML}$  is the thickness of the PML layer,  $h$  is the distance from the inner boundary of PML,  $R(0)$  is the theoretical reflection factor at normal incidence, and  $n$  is the type of the conductivity distribution.  $n = 2$  for parabolic conductivity.

The above procedure is followed in the case of the three dimensional case. Six components for the electric and magnetic fields are derived and Equations (3) and (4) can be reduced to three equations, in terms of the three scattered electric field components by eliminating the scattered magnetic field terms, which can then construct a linear set of equations. These final equations are used to construct a system of linear equations which can be written in the form  $Ax = y$ .  $A$  is a coefficient matrix,  $y$  is a vector related to the incident fields and  $x$  is the vector of unknown electric fields [10]. The number of cells in the 3D component domain is  $N = N_x x N_y x N_z$ . The matrix  $A$  is a sparse matrix of size  $(3N \times 3N)$  and  $x$  is a vector of size  $(3N \times 1)$ . Biconjugate gradients method is used to solve  $Ax = y$ .

### 3. NUMERICAL RESULTS

In this section, sample numerical results are presented to proof the validity of the developed formulation for computing the radar cross section (RCS) of a single cylinder coated with metamaterial, a linear array of coated cylinders are calculated and compared with the available data in the literature.

For 2D problems the radar cross section is given by [1]

$$\sigma = \lim_{\rho \rightarrow \infty} 2\pi\rho \frac{|\bar{E}^{scat}|^2}{|\bar{E}^{inc}|^2} \quad \text{for TM}_z \text{ case} \quad (9)$$

and

$$\sigma = \lim_{\rho \rightarrow \infty} 2\pi\rho \frac{|\bar{H}^{scat}|^2}{|\bar{H}^{inc}|^2} \quad \text{for TE}_z \text{ case} \quad (10)$$

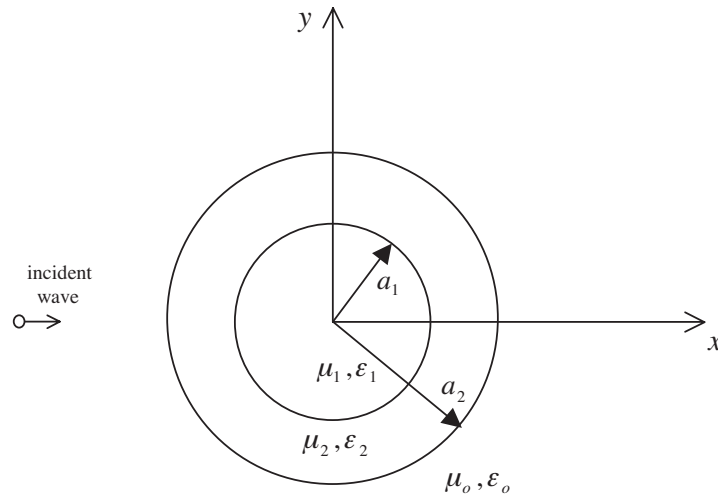


**Figure 1.** Geometry of 2D case.

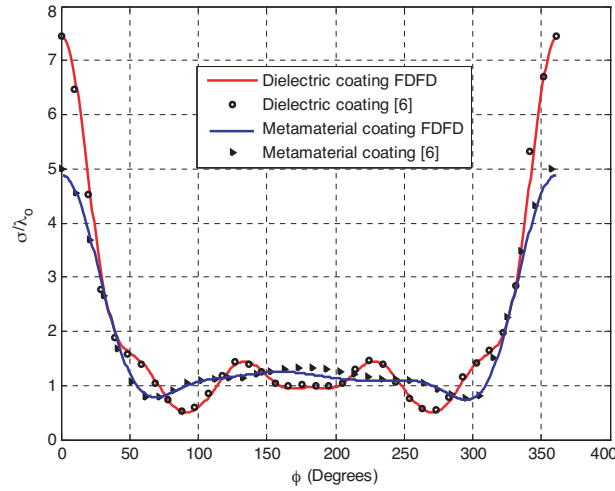
the geometry of the problem considered in 2D case is shown in Fig. 1.

The metamaterial parameters used in this paper are selectively used to provide confirmation of the validity of the new formulation by comparison of special cases with published results.

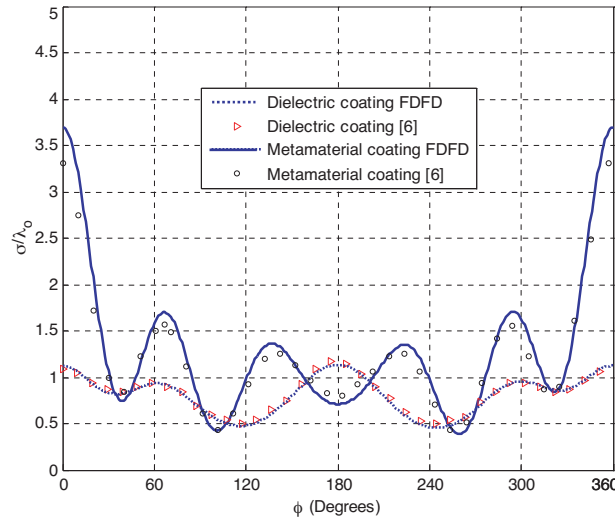
Figures 2, 3 show the computation of the RCS (TM and TE incidence) per unit length in case of a PEC (perfect electric conductor) cylinder coated by a DPS (Double Positive) or a DNG (Double Negative) layer, which is illuminated by a unit plane wave polarized along  $z$ -axis and propagating along  $x$ -axis (incidence angle is  $\theta_i = \pi$ ) where  $a_1 = 0.05$  m, and  $a_2 = 0.10$  m. The operating frequency is 1 GHz. The dielectric parameters are given by:  $\epsilon_2 = 9.8\epsilon_o$ , and  $\mu_2 = \mu_o$ , for the DPS case, and  $\epsilon_2 = -9.8\epsilon_o$ , and  $\mu_2 = -\mu_o$ , for the DNG case. It is observed that the RCS of TM incidence are of similar behavior: the both have large forward scattering. However, as shown in Fig. 2 for TE incidence, a cylinder coated with a conventional material has smaller forward scattering compared to a cylinder coated with a metamaterial. The results are in very good agreement with those obtained by Li and Shen [6].

Figure 4 shows the RCS of two layer dielectric ( $\epsilon_2 = 9.8\epsilon_o$ , and  $\mu_2 = \mu_o$ ) and metamaterial ( $\epsilon_2 = -9.8\epsilon_o$ , and  $\mu_2 = -\mu_o$ ) circular cylinder ( $a_1 = 0.05$  m,  $a_2 = 0.10$  m) illuminated by a TM plane wave at  $f = 300$  MHz and  $\theta = \pi$  compared with Matteo [15] and good agreement between those two results.

Figure 5 shows the radar cross section of a four layer superquadric



**Figure 2.** Bistatic RCS for a coated PEC circular cylinder ( $a_1 = 0.05$  m,  $a_2 = 0.10$  m) illuminated by a TM plane wave at  $f = 1$  GHz;  $\theta = \pi$  and material properties (DPS case: ( $\epsilon_2 = 9.8\epsilon_o$  and  $\mu_2 = \mu_o$ ); DNG case: ( $\epsilon_2 = -9.8\epsilon_o$  and  $\mu_2 = -\mu_o$ )).



**Figure 3.** Bistatic RCS for a coated PEC circular cylinder ( $a_1 = 0.05$  m,  $a_2 = 0.10$  m) illuminated by a TE plane wave at  $f = 1$  GHz;  $\theta = \pi$  and material properties (DPS case: ( $\epsilon_2 = 9.8\epsilon_o$  and  $\mu_2 = \mu_o$ ); DNG case: ( $\epsilon_2 = -9.8\epsilon_o$  and  $\mu_2 = -\mu_o$ )).



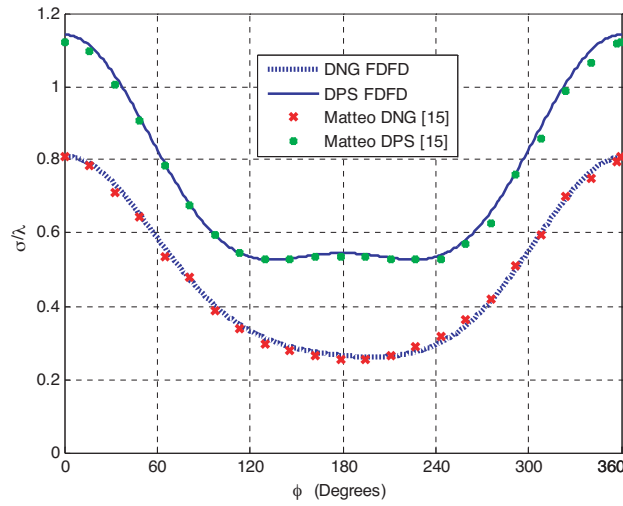


**Figure 4.** Bistatic RCS for two layer dielectric ( $\epsilon_2 = 9.8\epsilon_o$  and  $\mu_2 = \mu_o$ ) and metamaterial ( $\epsilon_2 = -9.8\epsilon_o$  and  $\mu_2 = -\mu_o$ ) circular cylinder ( $a_1 = 0.05$  m,  $a_2 = 0.10$  m) illuminated by a TM plane wave at  $f = 300$  GHz and  $\theta = \pi$ .

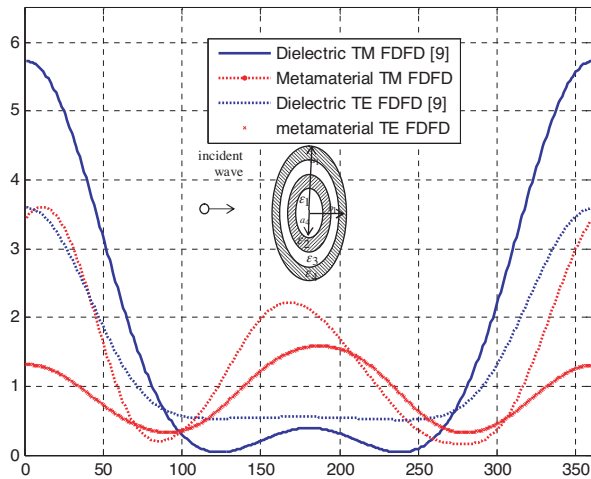


**Figure 5.** Radar cross section pattern of a four-layered cylinder ( $a_1 = 0.3\lambda$ ,  $a_2 = 0.25\lambda$ ,  $a_3 = 0.2\lambda$ ,  $a_4 = 0.15\lambda$ ), and  $b_i = a_i/2$ , ( $i = 1 : 4$ ),  $TM_z$  and  $TE_z$  plane wave for conventional and metamaterial ( $\theta = 0^\circ$ ,  $\phi = 0^\circ$ ).

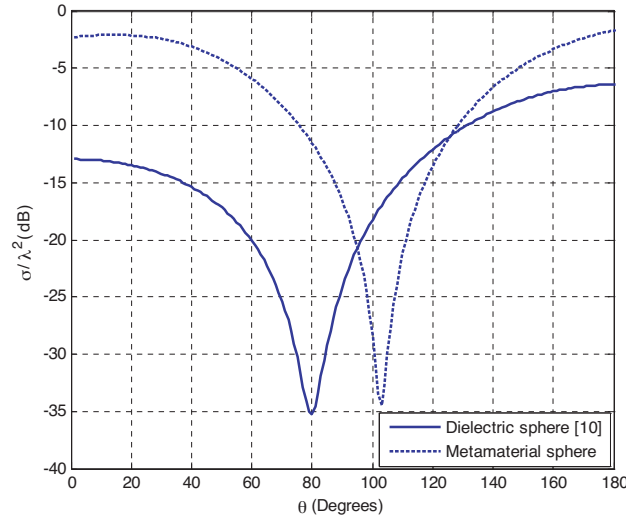


**Figure 6.** Bistatic RCS for dielectric and metamaterial sphere ( $\epsilon_r = \pm 4$ , radius = 0.5 m) at  $f = 100$  MHz.

cylinder with  $a_1 = 0.3\lambda$ ,  $a_2 = 0.25\lambda$ ,  $a_3 = 0.2\lambda$ ,  $a_4 = 0.15\lambda$ ,  $b_i = a_i/2$ , ( $i = 1 : 4$ ),  $\gamma = 2$ ,  $\epsilon_{r1} = 8$ ,  $\epsilon_{r2} = 6$ ,  $\epsilon_{r3} = 4$ , and  $\epsilon_{r4} = 2$  for either  $\text{TM}_z$  or  $\text{TE}_z$  incident plane wave and for metamaterial [9].

Figure 6 compares the bistatic RCS for a dielectric sphere ( $\epsilon_r = 4.5$ ,  $\mu_r = 1$ ,  $r = 0.5$  m), and for a metamaterial sphere ( $\epsilon_r = -4.5$ ,  $\mu_r = -1$ ,  $r = 0.5$  m) in the x-z plane with the resonance frequency is 100 MHz. The angle of incidences ( $\theta_i = 0^\circ$  and  $\varphi_i = 0^\circ$ ).

#### 4. CONCLUSIONS

The electromagnetic scattering from two- and three-dimensional objects coated with metamaterial are investigated. The FDFD method is used to formulate the problem. The radar cross sections from circular cylinder and multilayer elliptical cylinder, including DPS and DNG layers, have been considered. The scattering from the dielectric and metamaterial sphere are calculated. The results are compared with the available data in the literature. The scattering from the conducting and metamaterial sphere are depicted. The numerical results show that the level of the scattered field from these kinds of objects depends on the polarization of the incident wave and also on the operating frequency.

## REFERENCES

1. *IEEE Transaction on Antennas and Propagation Special Issue on Metamaterials*, Vol. 51, No. 10, Part I, Oct. 2003.
2. Caloz, C. and T. Itoh, *Electromagnetic Metamaterials: Transmission Line Theory and Microwave Applications*, John Wiley & Sons, Inc, New York, USA, 2006.
3. Eleftheriades, G. V., *Negative-Refractive Metamaterials*, 2005.
4. Markley, L. and G. V. Eleftheriades, "A negative-refractive-index metamaterial for incident plane waves of arbitrary polarization," *IEEE Antennas and Wireless Propagation Letters*, Vol. 6, 28–32, 2007.
5. Qiu, C.-W., H.-Y. Yo, S.-N. Burokur, S. Zouhdi, and L.-W. Li, "Electromagnetic scattering properties in a multilayered metamaterial cylinder," *IEIC Trans. Commun.*, Vol. E90-B, No. 9, 2423–2429, September 2007.
6. Li, C. and Z. Shen, "The electromagnetic scattering by a conducting cylinder coated with metamaterials," *Progress In Electromagnetics Research*, PIER 42, 91–105, 2003.
7. Shooshtari, A. and A. R. Sebak, "Electromagnetic scattering by parallel metamaterial cylinders," *Progress In Electromagnetics Research*, PIER 57, 165–177, 2006.
8. Henin, B. H., M. Al-Sharkawy, and A. Z. Elsherbeni, "Scattering of obliquely incident plane wave by array of parallel concentric metamaterial cylinders," *Progress In Electromagnetics Research*, PIER 77, 285–307, 2007.
9. Zainud-Deen, S. H., M. S. Ibrahim, and E. El-Deen, "A hybrid finite difference frequency domain and particle swarm optimization techniques for forward and inverse electromagnetic scattering problems", *The 23rd Annual Review of Progress in Applied Computational Electromagnetics*, Verona, Italy, March 19–23, 2007.
10. Zainud-Deen, S. H., E. El-Deen, and M. S. Ibrahim, "Electromagnetic scattering by conducting/dielectric objects," *The 23rd Annual Review of Progress in Applied Computational Electromagnetics*, Verona, Italy, March 19–23, 2007.
11. Henin, B. H., A. Z. Elsherbeni, and M. Al-Sharkawy, "Oblique incidence plane wave scattering from an array of circular dielectric cylinders," *Progress In Electromagnetics Research*, PIER 68, 261–279, 2007.
12. Henin, B. H., M. H. Al-Sharkawy, and A. Z. Elsherbeni, "Scattering of obliquely incident plane wave by an array of parallel

- concentric metamaterial cylinders,” *Progress In Electromagnetics Research*, PIER 77, 285–307, 2007.
13. Yee, K. S., “Numerical solution of initial boundary value problems using Maxwell’s equations in isotropic media,” *IEEE Trans. Antennas Propagat.*, Vol. 14, 302–307, May 1966.
  14. Berenger, J. P., “A perfectly matched layer for the absorption of electromagnetic waves,” *J. Comput. Phys.*, Vol. 144, 185–200, Oct. 1994.
  15. Pastorino, M., M. Raffetto, and A. Randazzo, “Interactions between electromagnetic waves and elliptically shaped metamaterials,” *IEEE Antennas and Wireless Propagation Letters*, Vol. 4, 165–168, 2005.